THE JOURNAL OF BIOLOGICAL CHEMISTRY VOL. 288, NO. 5, pp. 3112–3125, February 1, 2013

Adiponectin Receptors Form Homomers and Heteromers Exhibiting Distinct Ligand Binding and Intracellular Signaling Properties*[S]

Received for publication, July 25, 2012, and in revised form, December 18, 2012 Published, JBC Papers in Press, December 19, 2012, DOI 10.1074/jbc.M112.404624

Farid Almabouada[‡§], Alberto Diaz-Ruiz[‡§], Yoana Rabanal-Ruiz[‡§], Juan R. Peinado[¶], Rafael Vazquez-Martinez[‡§1], and Maria M. Malagon[‡§2]

From the [‡]Department of Cell Biology, Physiology, and Immunology, Instituto Maimonides de Investigacion Biomedica de Cordoba/University Hospital Reina Sofia, University of Cordoba, 14014 Cordoba, Spain, [§]CIBER Fisiopatologia de la Obesidad y Nutricion, Instituto de Salud Carlos III, Madrid, Spain, and the [¶]Department of Medical Sciences, University of Castilla la Mancha, 13071 Ciudad Real, Spain

Background: Adiponectin receptors (AdipoR1 and 2) mediate the effects of adiponectin, which possesses insulin sensitizing and anti-inflammatory properties.
Results: AdipoRs organize into oligomers exhibiting distinct interaction and signaling properties.
Conclusion: The cellular response to adiponectin depends on the specific AdipoR repertoire.
Significance: To envisage novel therapeutic strategies, the capacity of AdipoRs to form oligomeric complexes must be taken into consideration.

Adiponectin binds to two widely expressed receptors (AdipoR1 and AdipoR2) that contain seven transmembrane domains but, unlike G-protein coupled receptors, present an extracellular C terminus and a cytosolic N terminus. Recently, AdipoR1 was found to associate in high order complexes. However, it is still unknown whether AdipoR2 may also form homomers or heteromers with AdipoR1 or if such interactions may be functionally relevant. Herein, we have analyzed the oligomerization pattern of AdipoRs by FRET and immunoprecipitation and evaluated both the internalization of AdipoRs in response to various adiponectin isoforms and the effect of adiponectin binding to different AdipoR combinations on AMP-activated protein kinase phosphorylation and peroxisome proliferator-activated receptor α activation. Transfection of HEK293AD cells with AdipoR1 and AdipoR2 showed that both receptors colocalize at both the plasma membrane and the endoplasmic reticulum. Co-transfection with the different AdipoR pairs yielded high FRET efficiencies in non-stimulated cells, which indicates that AdipoR1 and AdipoR2 form homo- and heteromeric complexes under resting conditions. Live FRET imaging suggested that both homo- and heteromeric AdipoR complexes dissociate in response to adiponectin, but heteromers separate faster than homomers. Finally, phosphorylation of AMP-activated protein kinase in response to adiponectin was delayed in cells wherein heteromer formation was favored. In sum, our findings indicate that AdipoR1 and AdipoR2 form homo- and heteromers that present unique interaction behaviors and signaling properties. This raises the possibility that the pleiotropic, tissue-dependent functions of adiponectin depend on the expression levels of AdipoR1 and AdipoR2 and, therefore, on the steady-state proportion of homo- and heteromeric complexes.

The collagen-like, 30-kDa protein adiponectin (also known as acrp30, apM1, adipoQ, or GBP28) is the most abundantly secreted adipokine by adipose tissue (1, 2). Since its discovery in the mid-'90s (2–5), adiponectin has attracted much attention due to its role on the regulation of glucose and lipid metabolism in the liver, muscle, and fat and, thus, for its potential use for developing new treatment strategies aimed at tackling insulin resistance and type 2 diabetes, which are commonly linked to obesity (6). Specifically, adiponectin reduces hepatic gluconeogenesis, increases glucose uptake by muscle and adipocytes, and reduces liver and muscle triacylglyceride accumulation while increasing fatty acid oxidation in these tissues (6). Along with these insulin-sensitizing actions, adiponectin exhibits cardioprotective and anti-inflammatory properties by acting directly on cardiomyocites, vascular cells, and macrophages, which has been proposed to underlie its beneficial effects on cardiovascular disorders (7–10). Recent studies demonstrated that adiponectin also promotes cell survival of pancreatic β-cells (11) and may also play a role in the development and progression of distinct malignancies associated with obesity and insulin resistance, including breast cancer and colon cancer (12, 13). In fact, adiponectin circulating levels are reduced in obesity and inversely associated with the risk of developing type 2 diabetes, cardiovascular disease, and obesity-related cancers (13).

The diverse biological effects of adiponectin have been explained at least partly by the existence of different homo-oligomeric complexes of adiponectin (trimers, hexamers, and

* This work was supported by MINECO/FEDER (BFU2010-17116), J. Andalucia/FEDER (CTS-03039, CTS-6606), and CIBER Fisiopatologia de la Obesidad y Nutricion (Instituto de Salud Carlos III), Spain.
[S] This article contains a supplemental movie.
[1] To whom correspondence may be addressed: Dept. Cell Biology, Physiology, and Immunology, University of Cordoba, Campus Universitario Rabanales, 14014 Cordoba, Spain. Tel.: 34957218595; Fax: 34957218634; E-mail: bc2vamar@uco.es.
[2] To whom correspondence may be addressed: Dept. Cell Biology, Physiology, and Immunology, University of Cordoba, Campus Universitario Rabanales, 14014 Cordoba, Spain. Tel.: 34957218595; Fax: 34957218634; E-mail: bc1mapom@uco.es.

high molecular weight multimers) in plasma (14). Furthermore, adiponectin can exist as full-length (FLAdipoQ) or a smaller, globular fragment (GAdipoQ) generated by proteolytic cleavage of the former (15). These forms present distinct binding affinities to two adiponectin receptors identified so far, AdipoR1[3] and AdipoR2. These receptors, which share 67% amino acid identity, contain 7 transmembrane domains, but contrary to G protein-coupled receptors (GPCRs), their N terminus is intracellular and the C terminus is placed extracellularly (16). Although AdipoR1 expression is predominant in skeletal muscle and AdipoR2 is most abundantly expressed in the liver, both receptors are co-expressed in many cell types and tissues (17). It has been established that AdipoR1 and AdipoR2 have distinct functional signaling preferences (18). Thus, AdipoR1 action is mainly mediated by phosphorylation of AMP-activated protein kinase (AMPK), whereas AdipoR2 predominantly uses the peroxisome proliferator-activated receptor-α (PPARα) signaling pathway (18). At present, whether these signaling pathways are sufficient to explain the pleiotropic actions of adiponectin is a matter of debate. Actually, it has been shown that AdipoRs (mainly AdipoR1) are also capable of stimulating ERK1/2 phosphorylation through an Src/Ras-dependent pathway in HEK293 cells (19), phospholipase C/Ca^{2+}/calmodulin-dependent protein kinase pathway in myocytes and HeLa cells (20, 21), protein kinase CK2 in MCF7 cells (22), and ceramidase activity in pancreatic β-cells and cardiomyocytes in an AMPK-independent manner (11). Furthermore, a third membrane receptor, T-cadherin, has been shown to exhibit binding affinity for adiponectin in myocytes, endothelial cells, and smooth muscle but not in hepatocytes (23).

One major characteristic of both GPCR and tyrosine kinase receptor superfamilies is their ability to form multimeric complexes (homomers and heteromers) that differentially modulate discrete sets of signaling effectors upon activation by a given ligand (24, 25). In line with this, AdipoR1 has been recently shown to form homodimers in epithelial cells, endothelial cells, and myocytes (26). However, whether AdipoR2 may exist as homodimer/oligomer and/or form heteromeric complexes with AdipoR1 and how these interactions may affect adiponectin signaling is yet unknown. In this work we show that AdipoR1 and AdipoR2 form homo- and heteromers with similar efficiency that present unique interaction patterns and intracellular signaling kinetics upon adiponectin binding, which may contribute to the diverse tissue-specific actions exerted by this adipokine.

EXPERIMENTAL PROCEDURES

Reagents—Antibodies against calnexin and GFP were obtained from Abcam (Cambridge, UK), anti-EEA1 was from BD Transduction Laboratories, anti-LAMP1 from Enzo Life Sciences Inc. (Madrid, Spain), and anti-Na^+/K^+-ATPase was from Santa Cruz Biotechnology (Heidelberg, Germany). Polyclonal antibodies to AMPK and pAMPKα (Thr-172) were purchased from Cell Signaling Technology Inc. (Danvers, MA). Mouse anti-cMyc was from AbD Serotec (Oxford, UK), and anti-HisG, Alexa Fluor-conjugated secondary antibodies, and Lipofectamine 2000 were from Invitrogen. FM5–95 was from Molecular Probes (Barcelona, Spain), M-MuLV retro-transcriptase was from Fermentas GmbH (St. Leon-Rot, Germany), pECFP-C1, pEYFP-C1, pDsRed-Monomer-C1, and human pituitary cDNA library was from Clontech (Saint-Germain-en-Laye, France), and phrGFP-C1 was from Stratagene (La Jolla, CA). Full-length adiponectin (FLAdipoQ) and globular adiponectin (GadipoQ) were purchased from Biovendor GmbH (Heidelberg, Germany). Unless otherwise indicated, all other reagents were purchased from Sigma.

AdipoR1 and AdipoR2 Reporter Constructs—Total RNA from human pituitary cDNA library was reverse-transcribed into first-strand cDNA using the M-MuLV retro-transcriptase (Fermentas GmbH) according to the manufacturer's instructions. cDNAs corresponding to the encoding region of AdipoR1 and AdipoR2 were amplified using the following specific oligonucleotides: forward AdipoR1, 5′-gcttgtctaccatcagagg-3′; reverse AdipoR1, 5′-agactcttcctctcacttcag-3; forward AdipoR2, 5′-aagaaaggcttgggtatc-3′; reverse AdipoR2, 5′-ttctcagtcatgtaccacg-3. AdipoRs cDNAs were cloned directly into the T-vector (MBL, Cordoba, Spain) and subsequently subcloned in-frame with the C-terminal end of the ECFP, Venus-YFP (Clontech), phrGFP (Stratagene), and DsRed expression vectors (Clontech) or in-frame with the C-terminal end of the cMyc epitope tag in the pCMV-tag vector (kindly provided by Dr. Y. Anouar, European Institute for Peptide Research, University of Rouen). AdipoR1 and AdipoR2 with the hexahistidine tag were subcloned into pCDNA3.1(+) vector (Invitrogen) from pYES2/NTA and pYES2/NTB vectors (Invitrogen), respectively. Before use, all constructs were verified by sequencing (Genomic unit, SCAI, UCO, Spain).

Cell Culture and Transfection—HEK293AD cells were cultured in DMEM (Lonza, Basel, Switzerland) supplemented with 10% FBS (Invitrogen), 1% antibiotic-antimycotic solution (Sigma), and 2 mM L-glutamine (Sigma). For transient transfection experiments, cells were plated in 25-mm round coverslips at 6000 cells/cm^2, cultured for 48–72 h, and transfected with the corresponding expression vectors using Lipofectamine 2000 (Invitrogen) as recommended by the manufacturer.

Immunocytochemistry—Twenty-four hours after transfection, HEK293AD cells were fixed with 4% paraformaldehyde for 10 min, washed thoroughly, and incubated with PBS containing 0.3% Triton X-100 and 1% BSA for 1 h. Then, cells were exposed to anti-calnexin (1:200) or anti-EEA1 (1:500) primary antibodies overnight at 4 °C followed by Alexa488-, Alexa594-, or Alexa405-conjugated secondary antibodies (1:500) for 2 h at room temperature. Plasma membrane staining was assessed was by incubating transfected cells with 2 μM FM5–95 (Molecular Probes). Coverslips bearing the cells were then placed under a TCS-SP2-AOBS confocal microscope (Leica Corp., Heidelberg, Germany) fitted with a Plan-Fluar 63× oil immersion objective (n.a. = 1.4). Depending on the cell depth, 10–20 stacks per channel were collected, projected in a single image, and merged off-line. After acquisition, images underwent a deconvolution process with the software package HUYGENS

[3] The abbreviations used are: AdipoR, adiponectin receptor; GPCR, G protein-coupled receptor; AMPK, AMP-activated protein kinase; PPAR, peroxisome proliferator-activated receptor; ER, endoplasmic reticulum; ECFP, enhanced cyan fluorescent protein.

ESSENTIAL 2.4.4 (Scientific Volume Imaging, Hilversum, The Netherlands). Colocalization was examined by stack-by-stack visual inspection and considered as such when signals were coincident in the same planes.

Fluorescence Resonance Energy Transfer (FRET)—HEK293AD cells co-transfected with different combinations of ECFP-AdipoR1, Venus-YFP-AdipoR1, ECFP-AdipoR2, and Venus-YFP-AdipoR2 were fixed with 4% paraformaldehyde for 10 min and mounted in glycerol/PBS (1:1). Transfected cells were then transferred to the temperature-controlled stage of a Nikon Eclipse TE2000 microscope (Nikon, Tokyo, Japan) equipped with an ORCA-BT-1024G digital camera (Hamamatsu Photonics, Hamamatsu City, Japan) controlled by METAMORPH software (Universal Imaging Corp., West Chester, PA). Net FRET was assessed using the three-filter method (27). Three sequential images were acquired at 800-ms exposure with the suitable filters sets for donor (ECFP; excitation at 440 nm and emission at 510 nm), acceptor (Venus-YFP; excitation at 495 nm and emission at 540 nm), and FRET (excitation at 440 nm and emission at 540 nm) under a Plan Fluar 63× oil immersion objective (n.a. = 1.4). Raw FRET images were corrected with the Fully Specified Bleed Through (FSBT) method using the equation,

$$\text{FRET} - \text{raw FRET} - [\text{acceptor} - (\text{DA} \times \text{donor})] \times [\text{AF}] - [\text{donor} - (\text{AD} \times \text{acceptor})] \times [\text{DF}] \quad \text{(Eq. 1)}$$

where DA represents the contribution of the donor signal to the acceptor, AD is the contribution of the acceptor signal to the donor, AF represents the contribution of the acceptor to the raw FRET signal, and DF is the contribution of the donor signal to the raw FRET. These coefficients were calculated from cells expressing ECFP or Venus-YFP alone. To determine the FRET detection limit of the system, cells co-expressing ECFP and Venus-YFP proteins were measured. FRET efficiency was calculated in relation to a positive control consisting of a vector expressing ECFP and Venus-YFP in-frame and separated by 15 amino acids, which provided the upper FRET efficiency limit (50%). For image analysis and coefficient calculation, background was always subtracted in each image. A 1:1 Venus-YFP/ECFP ratio and equal Venus-YFP and ECFP intensities between all samples were used for FRET measurements.

Distances from interacting proteins were inferred from the empirically calculated FRET efficiencies according to the Förster's equation,

$$E = R_0^6/R_0^6 + r^6 \quad \text{(Eq. 2)}$$

where E is the FRET efficiency, R_0 is the Förster critical distance for the donor and acceptor probes used (4.9 nm for ECFP and Venus-YFP), and r is the donor-acceptor separation distance.

Confocal images were processed off-line using the PixFRET plug-in for IMAGEJ 1.41 (National Institute of Health, Bethesda, MA). This algorithm allows generation of normalized images of FRET (NFRET) and, hence, localization of protein-protein interactions within the cell by computing pixel by pixel the images of a sample acquired in a three-channel setting. These data were processed according to the formula and the methodology previously described (28–30).

Time-lapse FRET was monitored in living, transfected HEK293AD cells growing onto 25-mm round coverslips. Coverslips were mounted in a Sykes-Moore chamber and placed in the temperature-controlled stage of a fluorescence microscope (Nikon) fitted with a Plan Fluar 63× oil immersion objective (n.a. = 1.4). Images were acquired every 5 s for at least 4 min using the same Venus-YFP and ECFP filter sets and settings as mentioned above. After a 120-s image acquisition, prewarmed imaging medium supplemented with FLAdipoQ or GadipoQ (100 nM final concentration) was slowly pumped into the chamber. Changes in FRET were monitored as variations of the normalized Venus-YFP/ECFP ratio as described previously (31).

Immunoblotting—Total cell lysates were obtained in PBS buffer containing or not 5% β-mercaptoethanol (Roche Applied Science) and supplemented with complete protease inhibitor mixture (Roche Applied Science). A group of samples was boiled in the presence of β-mercaptoethanol (denaturing conditions), whereas another group was loaded in the SDS-PAGE gel without previous boiling and in the absence of β-mercaptoethanol (non-denaturing conditions). After gel electrophoresis, proteins were transferred to nitrocellulose membranes, and blots were blocked with 5% dry milk (Carl Roth GmbH, Karlsruhe, Germany) in Tris-buffered saline containing 0.05% Tween 20. Immunodetection was performed using anti-HisG (1:2500) or anti-GFP (1:2000) antibodies followed by incubation with horseradish peroxidase-conjugated goat anti-rabbit IgG or anti-mouse IgG (1:2,500) for 1 h at room temperature. Immunoreaction was visualized using ECL plus (GE Healthcare).

To investigate the presence of AdipoR monomers and dimers in the ER, we performed cell fractionation studies. Specifically, ER-microsome enriched fractions were obtained by sequential centrifugation. Total protein extracts from GFP-AdipoR1- or GFP-AdipoR2-transfected cells were centrifuged at 600 × *g* for 10 min, 15,000 × *g* for 5 min, and 100,000 × *g* for 60 min. The pellets from the second and third centrifugation cycles were loaded in a SDS gel and immunostained against the ER marker calnexin (1:200) and the plasma membrane marker Na^+/K^+-ATPase (1:400). Finally, the ER membrane-enriched fractions were processed in the presence or absence of β-mercaptoethanol and immunoblotted using anti-GFP (1:2000).

Immunoprecipitation—HEK293AD cells co-expressing cMyc-AdipoR1 and ECFP-AdipoR2 were lysed in Triton X-100 lysis buffer (50 mM Tris-HCl, 150 mM NaCl, 5 mM EDTA, 1% Triton X-100) containing complete protease inhibitor mixture. Cell lysates were cleared by centrifugation at 16,000 × *g*, and equal amounts of total protein per sample were incubated with 8 μg of anti-cMyc monoclonal antibody at 4 °C overnight. Immunocomplexes were collected with protein A-Sepharose (Invitrogen) by orbital incubation for 1 h and were then rinsed 3 times with lysis buffer. Immunoprecipitates were eluted with 0.1 M glycine buffer (pH 2.3) and immediately adjusted to pH 7.4 with Tris-HCl buffer. 50 μg of total cell lysate or 40 μl of eluted immunoprecipitates were boiled in Laemmli loading buffer with β-mercaptoethanol and immediately resolved in a 7.5% SDS-PAGE gel. Immunodetection was performed using anti-GFP (1:2000) or anti-cMyc (1:1000) antibodies followed by

incubation with horseradish peroxidase-conjugated anti-mouse IgG (1:2500) for 1 h at room temperature. Immunoreaction was visualized using ECL plus (GE Healthcare).

AdipoR Internalization—HEK293AD cells transfected with DsRed-AdipoR1 or DsRed-AdipoR2 were incubated in DMEM without FBS for 1 h and subsequently treated with 10^{-7} M FLAdipoQ or GAdipoQ for 0, 5, 30, and 60 min. Afterward, cells were fixed with 4% paraformaldehyde and immunostained with the early endosome marker EEA1 (1:500) or the lysosome marker LAMP1 (1:150). Another group of cells was co-transfected with the AdipoRs and a construct expressing HA-tagged transferrin receptor as a marker of the recycling pathway and then immunostained against HA (1:200). At least 10 confocal images per experimental group were collected. The colocalization rate between AdipoR and EEA1, LAMP1, or transferrin receptor fluorescent signals was estimated off-line by calculating the Pearson's coefficient with IMAGEJ 1.41 software (National Institute of Health). This is a value computed to be between −1 and 1, with −1 being no overlap between images whatsoever and 1 being perfect image registration.

Evaluation of AMPK Phosphorylation—Twenty-four hours after transfection with cMyc-AdipoR1, cMyc-AdipoR2, or cMyc-AdipoR1/His_6G-AdipoR2, cells were preincubated with FBS-free DMEM for 1 h and subsequently incubated in the absence or presence of 100 nM FLAdipoQ for 0, 5, 15, and 30 min. Treated cells were lysed with lysis buffer (62.5 mM Tris-HCl, 2% sodium dodecyl sulfate, 20% glycerol, 100 mM dithiothreitol, and 0.005% bromphenol blue). Whole-cell lysates were separated in a 10% SDS-PAGE gel, transferred to nitrocellulose membranes, and stained with Ponceau S for visualization of protein bands and confirmation of equal protein loading for further comparative analysis. Then membranes were sequentially incubated with rabbit anti-phospho-AMPKα (Thr172) (1:1000) or total AMPK (1:1000) and horseradish peroxidase-conjugated, goat anti-rabbit IgG (1:2500). Densitometric analysis of bands was carried out with IMAGEJ 1.41 software. Quantitative data from immunoreactive bands revealed with anti-phospho-AMPK serum were normalized to the corresponding total AMPK values.

Bioluminescence Imaging—Human HepG2 hepatocarcinoma cells were transfected with either DsRed-AdipoR1, DsRed-AdipoR2, or GFP-AdipoR1/DsRed-AdipoR2 in combination with a luciferase reporter construct driven by multiple PPAR response elements (DR-1) (a generous gift of Dr. Kim from Seoul National University, Korea). After 24 h, transfected cells were incubated with 0.2 mM luciferin for 30 min and then placed in the temperature-controlled stage of an inverted microscope (Nikon Eclipse TE2000 microscope) equipped with a photon-counting camera system (Hamamatsu Photonics) under the control of WASABI software (Hamamatsu Photonics). The system was set to accumulate photons during 10-min intervals for 40 min (base line). Afterward, cells were exposed to 100 nM FLAdipoQ, and photon counting was resumed for another 60 min in the presence of the treatment. DsRed and GFP fluorescent images were acquired before the experiment to confirm the expression of AdipoRs in the cells imaged.

Statistical Analysis—Data from HEK293AD cells were obtained from a minimum of three replicate wells per treatment from at least three independent experiments. Multiple comparisons were assessed by one-way analysis of variance followed by a Newman-Keuls Multiple Comparison test using GraphPad Prism 4 (GraphPad Software, Inc., La Jolla, CA). Differences were considered statistically significant if $p < 0.05$.

RESULTS

Subcellular Localization of AdipoR1 and AdipoR2 Recombinant Proteins—AdipoR1 and AdipoR2 genes were cloned from human pituitary, and each cDNA was inserted into a pcDNA3 vector in tandem with sequences coding for different tag proteins (*i.e.* phrGFP, ECFP, Venus-YFP, and DsRed as well as His_6 and c-Myc) in the cytosolic N-terminal region of the receptors. These constructs were tested for plasma membrane targeting by cell transfection and subsequent confocal microscopy visualization. In all cases, chimera proteins were found in the plasma membrane of HEK293AD cells. Shown in Fig. 1*A* are representative confocal micrographs of HEK293AD cells expressing DsRed-AdipoR1 (*left panel*) or DsRed-AdipoR2 (*right panel*) in which fluorescent signals outline the cell surface. Furthermore, plasma membrane labeling with the lipophilic marker FM5–95 in cells transfected with GFP-AdipoR1 or GFP-AdipoR2 unveiled a significant overlapping of both fluorescent signals (Fig. 1*B*), which confirms that these chimera proteins are correctly targeted to the plasma membrane in these cells. Similarly, ECFP and Venus-YFP variants of both receptors were also present in the cell surface (data not shown), which ensures that tagging of their N-terminal domains with the different reporter proteins does not hinder receptor intracellular trafficking. In addition to the plasma membrane, transfected AdipoR1 and AdipoR2 also distributed to tubulovesicular structures. Immunolabeling of GFP-AdipoR1- or GFP-AdipoR2-expressing cells with the ER marker calnexin revealed a high degree of co-localization in this compartment (Fig. 1*C*), suggesting that the recombinant receptors are retained in the ER during their synthesis or intracellular transport. Nevertheless, we cannot exclude the possibility that ER accumulation of AdipoRs might be caused by CMV-promoter driven overexpression of these proteins.

When HEK293AD cells were co-transfected with the two receptors tagged with different fluorescent markers (GFP-AdipoR1 and DsRed-AdipoR2) and visualized by confocal microscopy, strong co-localization between both fluorescent signals at the plasma membrane and the ER was observed (Fig. 2). This suggested that when the receptors are co-expressed, they could interact physically.

AdipoR1 and AdipoR2 Homo- and Heteromerization—FRET was chosen to analyze AdipoR oligomerization in HEK293AD cells. The ability and efficiency of AdipoR1 and AdipoR2 to form homomers were first evaluated by transfecting cells with the FRET pairs ECFP-AdipoR1/Venus-YFP-AdipoR1 or ECFP-AdipoR2/Venus-YFP-AdipoR2. Twenty-four hours after transfection, fluorescent signals were collected on a wide-field fluorescence microscope calibrated for FRET stoichiometry. As FRET controls, groups of cells were co-transfected with the ECFP and Venus-YFP vectors (negative control) or with a vector coding for both fluorescent proteins in tandem and separated by 15 amino acids (positive control), which translates into

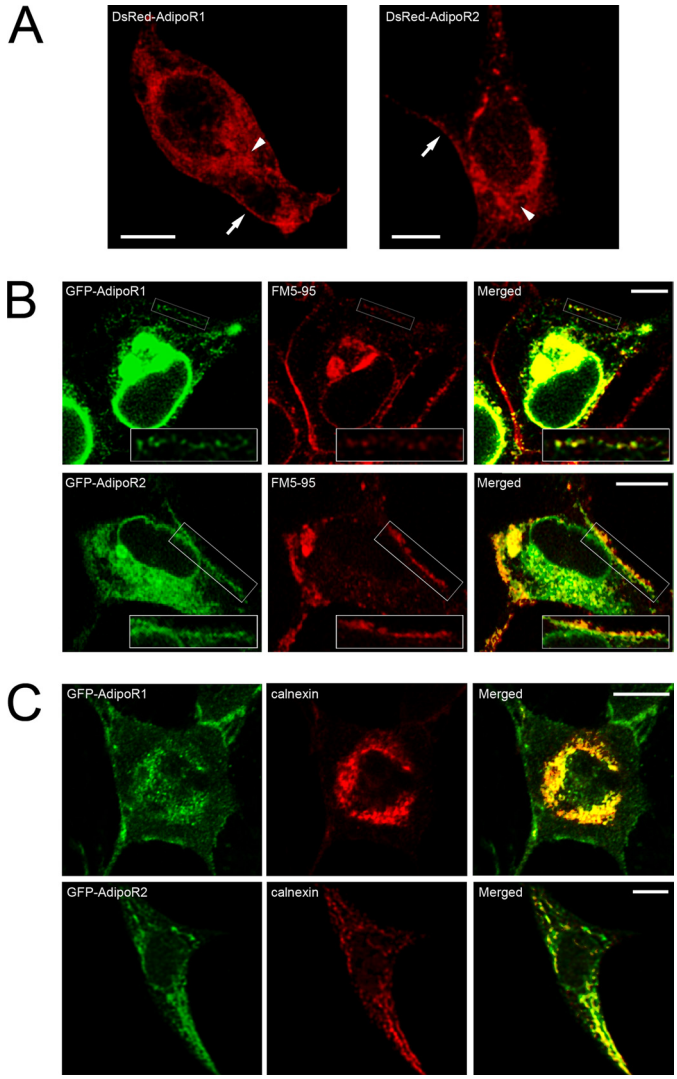

FIGURE 1. **Intracellular localization of fluorescently tagged AdipoR1 and AdipoR2 in HEK293AD cells.** *A*, representative confocal images of HEK293AD cells expressing DsRed-AdipoR1 (*left panel*) or DsRed-AdipoR2 (*right panel*) are shown. AdipoR1 and AdipoR2 fluorescent signals accumulate in close apposition to the plasma membrane (*arrows*) as well as in an intracellular compartment surrounding the nucleus (*arrowheads*). *B*, shown is colocalization of GFP-AdipoR1 or GFP-AdipoR2 (*green*) with the plasma membrane marker FM5–95 (*red*). As shown in the *rightmost panels*, both AdipoR1 and AdipoR2 signals exhibit significant overlapping with FM5–95 at the plasma membrane. *C*, shown is colocalization analysis of GFP-tagged AdipoR1 and AdipoR2 (*green*) with the ER marker calnexin (*red*). Intracellular accumulation of AdipoR1 and AdipoR2 strongly coincides with calnexin immunosignal. *Scale bars*, 5 μm.

a separation distance (Förster's distance) between donor and acceptor that yields the maximum FRET efficiency (50%; Fig. 3*A*). Use of the AdipoR1 or AdipoR2 FRET pairs yielded FRET efficiencies significantly higher than that obtained with the negative control (Fig. 3*A*), which demonstrated that adiponectin receptors are able to form homomeric complexes. We then explored whether these receptors are also able to form heteromeric structures. To this end, FRET efficiency in cells co-expressing ECFP-AdipoR1/Venus-YFP-AdipoR2 or ECFP-AdipoR2/Venus-YFP-AdipoR1 was measured. In both cases, FRET efficiencies were also significantly higher than that yielded by the negative control (Fig. 3*A*), which indicated that adiponectin receptors can also assemble into heteromeric complexes. Specifically, theoretical FRET efficiency monitored for the homomers (AdipoR1, AdipoR2) and heteromers (AdipoR1-AdipoR2) were 15.5, 12.7, and 14.8%, respectively. Given that all the pairs of FRET constructs (CFP/CFP, YFP/YFP, and CFP/YFP) have the same probability to occur, these data indicate that most AdipoRs (76.5–93.4%) would form dimers. Considering Förster's distance parameters, the theoretical distance between interacting AdipoR1 monomers was 6.91 $\pm$ 0.13 nm, for AdipoR2 was 7.46 $\pm$ 0.19 nm, and for interaction of AdipoR1 and AdipoR2 was 7.09 $\pm$ 0.15 nm or 6.99 $\pm$ 0.12 nm depending on the FRET pair used. These calculated distances are consistent with the distance accessible by the FRET technique (between 2 and 10 nm) and are comparable with the diameters of most biological molecules (32).

To reveal the subcellular localization of adiponectin receptor interaction, confocal images of HEK293AD cells expressing the different FRET constructs were processed using PixFRET. This approach revealed that regardless of the FRET pair used, receptor interaction occurred mainly at the plasma membrane level (Fig. 3*B*). In addition, although to a lesser extent, some intracellular regions likely corresponding to the ER compartment were also positive (Fig. 3*B*), suggesting that AdipoR interactions may begin in early compartments of the secretory pathway. This observation was further supported by subcellular fractionation experiments (see below).

To further substantiate that AdipoRs are able to form complexes, protein extracts from His_6-AdipoR1- or ECFP-AdipoR2-transfected HEK1293AD cells were subjected to non-denaturing gel electrophoresis. When protein extracts were incubated with the reducing agent β-mercaptoethanol and immunoblotted using antibodies against the tag molecules (anti-HisG and anti-GFP), single immunoreactive bands of ~45 and ~70 kDa corresponding to exogenous AdipoR1 and AdipoR2, respectively, were revealed (Fig. 3*C*, *left lanes*). Alternatively, when the native conformation of the receptors was preserved by omission of β-mercaptoethanol, the monomeric forms of the receptors (*i.e.* His_6-AdipoR1 (~45 kDa) and CFP-AdipoR2 (~70 kDa)) as well as forms of higher molecular masses were detected. The estimated molecular weights of these additional forms are concordant with the theoretical molecular weights of homodimeric and multimeric complexes (Fig. 3*C*, *middle lanes*).

Protein extracts from cells co-transfected with cMyc-AdipoR1 and ECFP-AdipoR2 were also collected and immunoprecipitated using an anti-cMyc monoclonal antibody. As shown in Fig. 3*D*, when cMyc-AdipoR1 was immunoprecipitated with -cMyc, ECFP-AdipoR2 was co-immunoprecipitated, indicating that AdipoR1 and AdipoR2 exist in a protein complex in cMyc-AdipoR1/ECFP-AdipoR2-co-expressing cells under basal conditions.

To test whether AdipoR oligomerization takes place in the ER, protein extracts from GFP-AdipoR1- or GFP-AdipoR2-expressing cells were sequentially centrifuged and electrophoresed under reducing or non-reducing conditions. As shown in Fig. 3*E*, the microsomal fraction (P2) was enriched in the ER marker calnexin and lacked immunosignal for the plasma membrane marker Na^+/K^+-ATPase, which separated in the previous centrifugation step (P1). ER-membrane enriched frac-

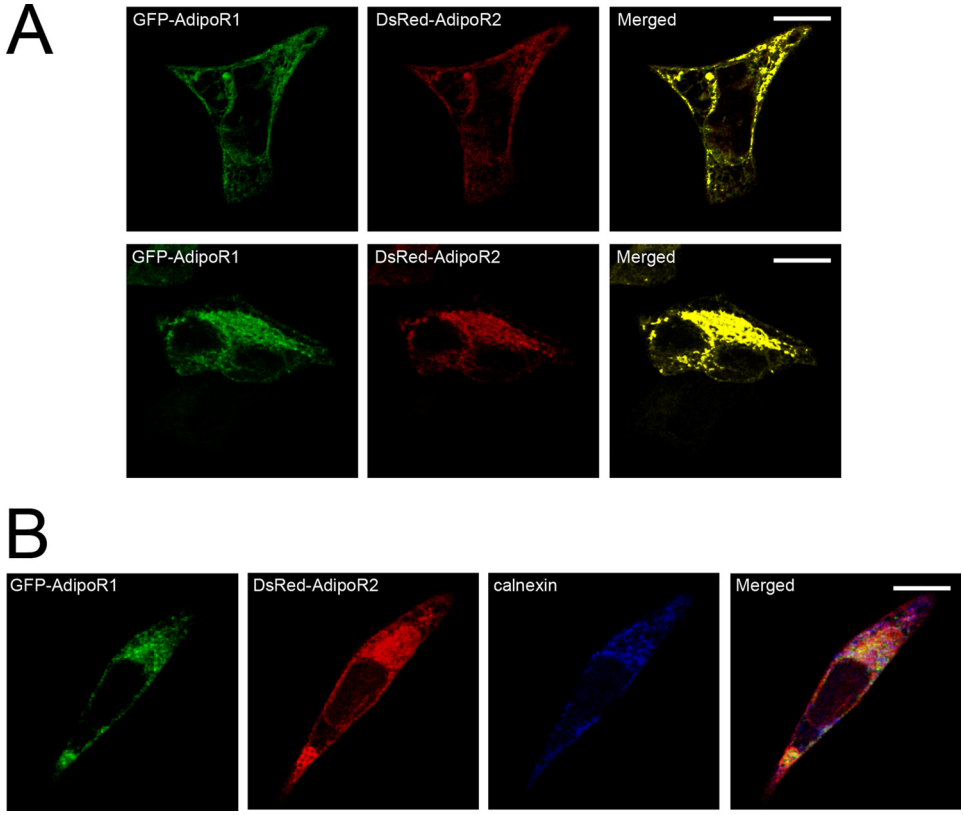

FIGURE 2. **Colocalization of exogenously expressed AdipoR1 and AdipoR2.** *A*, co-transfection of HEK293AD cells with GFP-AdipoR1 (*green*) and DsRed-AdipoR2 (*red*) reveals a high degree of colocalization along the plasma membrane (*top panels*) as well as in the ER (*bottom panels*). *B*, triple fluorescence detection of GFP-AdipoR1 (*green*), DsRed-AdipoR2 (*red*), and the ER marker calnexin (*blue*) is shown. Colocalization of the three markers was found intracellularly within the ER, whereas overlapping of AdipoR1 and AdipoR2 also occurred at the plasma membrane.

tions were examined for the presence of AdipoR monomers and multimeric complexes. Thus, in protein extracts incubated with β-mercaptoethanol, single immunoreactive bands of ~70 kDa corresponding to exogenous GFP-AdipoR2 or GFP-AdipoR2 were revealed (Fig. 3*F*, *left lanes*). On the other hand, in the absence of β-mercaptoethanol the monomeric forms of the receptors (~70 kDa) as well as forms of higher molecular masses likely corresponding to AdipoR1 and AdipoR2 complexes were detected (Fig. 3*F*, *right lanes*).

We next assessed the effect of FLAdipoQ and GAdipoQ on the dynamics of AdipoR1 and AdipoR2 homo- and heteromerization. To this end, we carried out simultaneous real-time measurements of ECFP and Venus-YFP fluorescence in single, living cells expressing different combinations of FRET pairs. Fig. 4*A* shows representative examples of ECFP and Venus-YFP fluorescence recording over time in cells expressing the different AdipoR FRET constructs and treated with either 100 nM FLAdipoQ (*top panels*) or 100 nM GAdipoQ (*bottom panels*). Irrespective of the adiponectin form administered, ECFP fluorescent emission increased, whereas Venus-YFP fluorescence concomitantly decreased (Fig. 4*A*). This decrease in FRET signals could be due to adiponectin-induced conformational changes within the AdipoR complexes. These data are also compatible with the idea that ligand binding induces the dissociation of the AdipoR complexes as has been suggested to occur for several GPCRs (33, 34). In line with this, exposure of AdipoR-transfected cells to adiponectin caused a time-dependent increase in the monomeric forms of AdipoRs and a concomitant decrease in the amount of oligomeric forms (data not shown). In this scenario our FRET data suggest that the time-course of AdipoR dissociation induced by GAdipoQ is similar for all AdipoR pairs (7.78 ± 1.57 s for AdipoR1 homomers, 6.07 ± 0.80 s for AdipoR2 homomers, and 5.33 ± 0.41 s for AdipoR1/AdipoR2 heteromers; Fig. 4*B*). On the other hand, FLAdipoQ-induced dissociation of AdipoR1/AdipoR1 (18.67 ± 4.53 s) and AdipoR2/AdipoR2 homomers (15.50 ± 3.37 s) was slower than that induced by GAdipoQ (Fig. 4*B*). Interestingly, when formation of AdipoR1/AdipoR2 heteromers was favored by co-expression of the corresponding constructs and cells were treated with FLAdipoQ, heteromer dissociation was significantly accelerated, reaching a peak at 5.09 ± 0.10 s (Fig. 4*B*).

The time-course of AdipoR reassociation (and/or recovery of the original conformation) was also estimated by measuring the time required to recover base-line levels of the Venus-YFP/ECFP ratio. No significant differences regarding the effect of FLAdipoQ and GAdipoQ on homo- or heteromer reassociation were found (Fig. 4*C*). However, irrespective of the pair of constructs examined, receptor reassociation resulted about 2-fold slower in response to FLAdipoQ treatment than to GAdipoQ (Fig. 4*C*).

AdipoR1 and AdipoR2 Internalization Dynamics in Response to Adiponectin—To evaluate the effects of FLAdipoQ and GAdipoQ on AdipoR1 and AdipoR2 internalization dynamics, DsRed-AdipoR1- or DsRed-AdipoR2-transfected cells were serum-starved for 1 h and challenged with 100 nM FLAdipoQ or

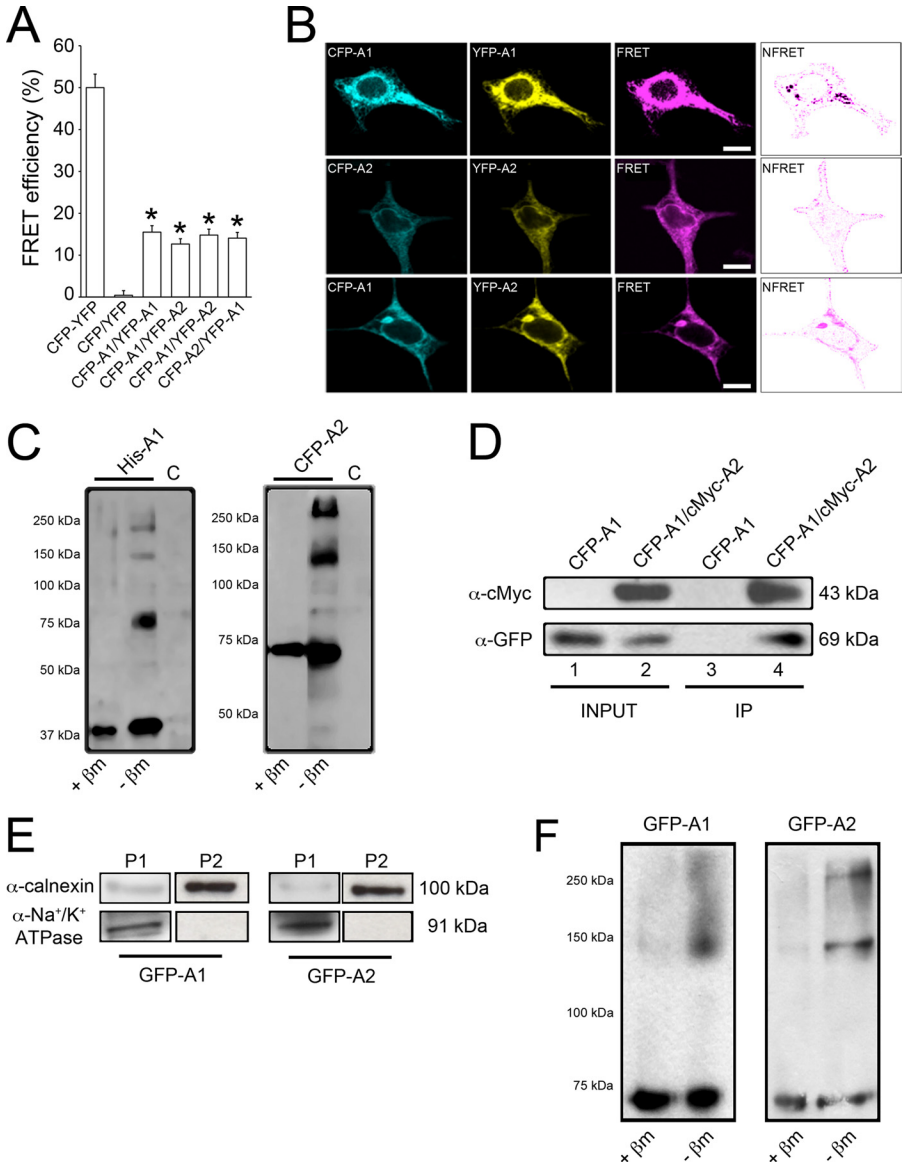

FIGURE 3. **Evaluation of AdipoR1 and AdipoR2 interaction.** *A*, shown are measurements of FRET efficiency in fixed HEK293AD cells transfected with different ECFP and Venus-YFP constructs. FRET efficiency values were calculated as described under "Experimental Procedures." Cells expressing ECFP and Venus-YFP coupled in-frame within the same plasmid construct were used as the positive control (46 cells). Cells expressing ECFP and Venus-YFP empty vectors were used as negative control (44 cells). FRET was measured in cells co-transfected with ECFP-AdipoR1/Venus-YFP-AdipoR1 (71 cells), ECFP-AdipoR2/Venus-YFP-AdipoR2 (67 cells), ECFP-AdipoR1/Venus-YFP-AdipoR2 (63 cells), or ECFP-AdipoR2/Venus-YFP-AdipoR1 (62 cells) under basal culture conditions. Only cells displaying Venus-YFP/ECFP ratios close to or equal to 1 were included in the analysis. Results presented are the average ± S.E. of the number of cells indicated (*, $p < 0.001$ *versus* negative control). *B*, shown is a PixFRET map of FRET efficiencies yielded by AdipoR homo- and heteromers. Normalized FRET (*NFRET*) channels (*rightmost panels*) reveal that protein interaction occurs mainly at the plasma membrane, although some positive signal is also present in the ER. *Scale bars*, 5 μm. *C*, protein extracts from HEK293AD cells were transfected with His_6-tagged AdipoR1 (*left panel*) or ECFP-tagged AdipoR2 (*right panel*) and electrophoresed in the presence or absence of the reducing agent β-mercaptoethanol. As the control (*C*), cells were transfected with a construct coding for the His_6 tag alone. *D*, immunoprecipitation (*IP*) of the AdipoR1/AdipoR2 complex is shown. Immunoprecipitation was carried out with lysates prepared from HEK293AD cells co-expressing the ECFP-AdipoR1/cMyc-AdipoR2 combination. For control purposes, HEK293AD cells were transfected with ECFP-AdipoR1 alone. After cell lysis, protein extracts were immunoprecipitated with monoclonal anti-cMyc antibody and then immunoblotted using anti-cMyc or anti-GFP polyclonal antibodies. Monoclonal anti-cMyc antibody co-precipitated ECFP-AdipoR2 in ECFP-AdipoR1/cMyc-AdipoR2 co-expressing cells (*lane 4*) but not in cells expressing ECFP-AdipoR1 alone (*lane 3*). *E*, assessment of ER membrane-enriched protein extracts by subcellular fractionation is shown. Protein extracts from GFP-AdipoR1- or GFP-AdipoR2-transfected cells were centrifuged at 600 × *g* for 10 min, 15,000 × *g* for 5 min, and 100,000 × *g* for 60 min. Pellets from the second (*P1*) and third (*P2*) centrifugation steps were immunostained against the ER membrane marker calnexin (*top panels*) and the plasma membrane marker Na^+/K^+-ATPase (*bottom panels*). *F*, subcellular fractionation of HEK293AD cell extracts was performed to further investigate the presence of AdipoR complexes in ER membrane-enriched fractions. ER-enriched fractions were incubated in the presence or absence of β-mercaptoethanol (*βm*), electrophoresed, and immunostained against GFP to identify AdipoR monomers and multimers.

100 nM GAdipoQ for 0, 5, 30, and 60 min. Afterward, cells were fixed and immunostained for the early endosome marker EEA1. AdipoR1 internalization, which was estimated as the co-localization index between DsRed-AdipoR1 and EEA1 fluorescent signals, was significantly increased after a 5-min exposure to FLAdipoQ (Fig. 5, *A* and *B*). The co-localization rate between AdipoR1 and EEA1 returned to basal levels after longer exposure times (30 and 60 min). On the other hand, significant co-localization of the two fluorescence emission signals only occurred at 30 min after GAdipoQ treatment (Fig. 5, *A* and *B*).

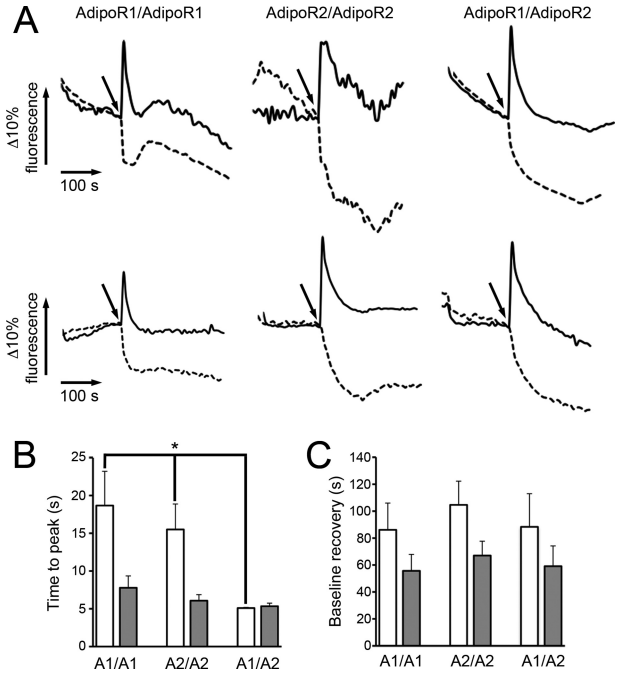

FIGURE 4. **Live FRET imaging.** *A*, shown are time-lapse recordings of ECFP (*solid lines*) and Venus-YFP (*dashed lines*) fluorescent signals in single, living HEK293AD cells co-transfected with the different combinations of FRET constructs. ECFP and Venus-YFP fluorescent emissions were monitored under non-stimulated conditions (*base line*) for 120 s. Afterward, cells were treated with 100 nM FLAdipoQ (*top panels*) or 100 nM GAdipoQ (*bottom panels*), and fluorescence was recorded for an additional 200-s period. *B*, shown is the average time for the Venus-YFP/ECFP ratio to attain its minimal value after adiponectin administration. *C*, shown is the average time for Venus-YFP/ECFP ratio to regain values close to base line after adiponectin administration. Data correspond to representative examples of FRET profiles from cells exposed to FLAdipoQ and GAdipoQ ($n = 15$, 10, and 11 cells for AdipoR1 pairs, AdipoR2 pairs, and AdipoR1-AdipoR2 pairs, respectively, in experiments with FLAdipoQ; $n = 18$, 14, and 7 cells for AdipoR1 pairs, AdipoR2 pairs, and AdipoR1-AdipoR2 pairs, respectively, in experiments with GAdipoQ; $n = 5$ and 6 separate experiments for FLAdipoQ and GAdipoQ, respectively). *, $p < 0.001$ *versus* ECFP-AdipoR1/Venus-YFP-AdipoR1 and ECFP-AdipoR2/Venus-YFP-AdipoR2-expressing cells.

We found that, similar to that observed for AdipoR1, internalization of AdipoR2 significantly increased after a 5-min treatment with FLAdipoQ, whereas it increased after a 30-min exposure to GAdipoQ (Fig. 5, *C* and *D*). Altogether, these findings demonstrate that both FLAdipoQ and GAdipoQ trigger AdipoR1 and AdipoR2 internalization. However, GAdipoQ-induced AdipoR1 and AdipoR2 internalization was delayed as compared with that induced by FLAdipoQ. The supplemental movie shows an example of FLAdipoQ-induced adiponectin receptor internalization tracked by fluorescence videomicroscopy. As shown in the movie, upon adiponectin stimulation DsRed-AdipoR1 was detected in very mobile, vesicle-like structures that displayed lateral movements along the plasma membrane or retrograde transport.

To further characterize the internalization dynamics of AdipoRs, AdipoR1- and AdipoR2-transfected cells were immunostained for markers of recycling endosomes (transferrin receptor) and lysosomes (LAMP1) after the administration of GAdipoQ or FLAdipoQ for 0, 5, 30, and 60 min. Both GAdipoQ and FLAdipoQ induced the co-localization of AdipoRs with LAMP1 but only after a 60-min exposure to the treatment (Fig. 5, *E*—*H*). In the particular case of AdipoR1-expressing cells treated with FLAdipoQ, the increase in the co-localization rate was observed after 30 min in the presence of the ligand (Fig. 5*F*). Altogether, these results are consistent with the localization of AdipoRs in the early endosomal compartment at earlier times and suggest that irrespective of the treatment, after 30–60 min of ligand binding an important proportion of the receptors is directed toward the lysosomal compartment for protein degradation.

On the other hand, although AdipoRs exhibited some overlap with transferrin receptor under non-stimulated conditions, we did not find significant co-localization after GAdipoQ or FLAdipoQ administration (Fig. 6), which suggests that the receptors are not recycled to the plasma membrane after ligand-induced activation and internalization.

Influence of AdipoR1 and AdipoR2 Interaction on AMPK Phosphorylation and PPARα Activation—We next assessed the functional consequences of the expression of different combinations of adiponectin receptors by measuring AMPK phosphorylation levels and PPARα activation in response to FLAdipoQ. Specifically, treatment of AdipoR1-expressing HEK293AD cells with 100 nM FLAdipoQ caused a rapid, robust, and transient increase in AMPK phosphorylation. Specifically, the pAMPK/AMPK ratio increased by 190% at 5 min and returned to base-line levels at 15 min after FLAdipoQ administration (Figs. 7, *A* and *B*, *left panels*). In cells transfected with AdipoR2 alone, FLAdipoQ was unable to modify basal phosphorylation of AMPK at any time point tested (Fig. 7, *A* and *B*, *middle panels*). Finally, AMPK phosphorylation levels increased in response to FLAdipoQ administration in AdipoR1/AdipoR2 co-expressing cells. However, in contrast to that found in AdipoR1-transfected cells, the effect was only patent after a 30-min exposure to the adipokine (Figs. 7, *A* and 7*B*, *right panels*). In sum, these findings indicate that the time-course of FLAdipoQ-induced AMPK phosphorylation is different depending on the predominance of homomeric or heteromeric AdipoRs.

PPARα activation was evaluated in a human hepatocarcinoma cell line (HepG2 cells) as its transcriptional activity on a luciferase reporter driven by multiple PPAR response elements (DR-1). Thus, treatment of AdipoR1-transfected HepG2 cells with FLAdipoQ for 1 h did not increase the capacity of PPARα to activate the DR-1-driven luciferase expression, whereas it significantly increased photon emission in AdipoR2-expressing cells (Fig. 7*C*). Interestingly, in cells co-expressing both receptors, FLAdipoQ treatment enhanced luciferase expression similarly to that found in cells expressing AdipoR2 alone (Fig. 7*C*).

DISCUSSION

Receptor oligomerization is a key process that helps modulate and diversify the functional effects of receptor ligands. Tyrosine kinase receptors, such as insulin or EGF receptors, have long been known to associate into dimers that are required to initiate the corresponding receptor-mediated signaling (for review see Ref. 24). More recently, oligomerization of seven-transmembrane domain GPCRs has emerged as a widespread mechanism for fine-regulation of GPCR function (35–37). During the isolation and characterization of the AdipoRs,

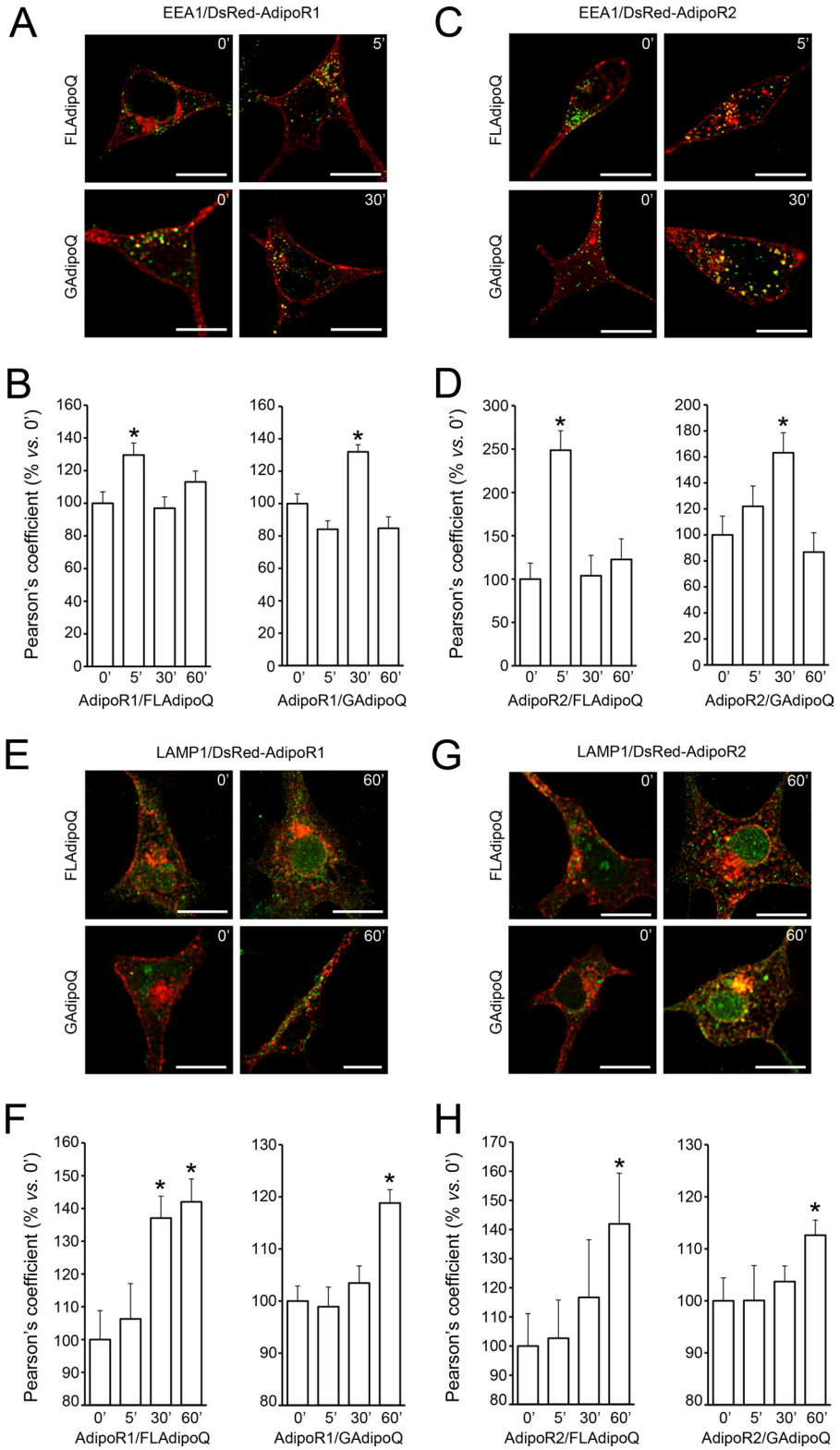

FIGURE 5. **AdipoR1 and AdipoR2 internalization dynamics in response to adiponectin.** *A* and *C*, shown are representative confocal images of HEK293AD cells expressing DsRed-AdipoR1 (*A*) or DsRed-AdipoR2 (*C*) and treated with 100 nM FLAdipoQ (*left panels*) or 100 nM GAdipoQ (*right panels*) for 0, 5, 30, and 60 min. After treatment, cells were fixed and immunostained against the early endosome marker EEA1 (*green*). *B* and *D*, shown is quantification of the colocalization index (Pearson's coefficient) between DsRed-AdipoR1 or DsRed-AdipoR2 and EEA1 immunofluorescent signal in FLAdipoQ (*left graphs*)- or GAdipoQ-treated cells (*right graphs*). *E* and *G*, representative confocal images of HEK293AD cells expressing DsRed-AdipoR1 (*E*) or DsRed-AdipoR2 (*G*) treated with 100 nM FLAdipoQ (*left panels*) or 100 nM GAdipoQ (*right panels*) for 0, 5, 30, and 60 min and immunostained against LAMP1 (*green*). *F* and *H*, shown is the colocalization index between DsRed-AdipoR1 or DsRed-AdipoR2 and LAMP1 in FLAdipoQ (*left graph*)- or GAdipoQ-treated cells (*right graph*). Data are represented as the average ± S.E. from at least 12 cells per group collected from three independent experiments. *, $p < 0.05$ *versus* untreated cells.

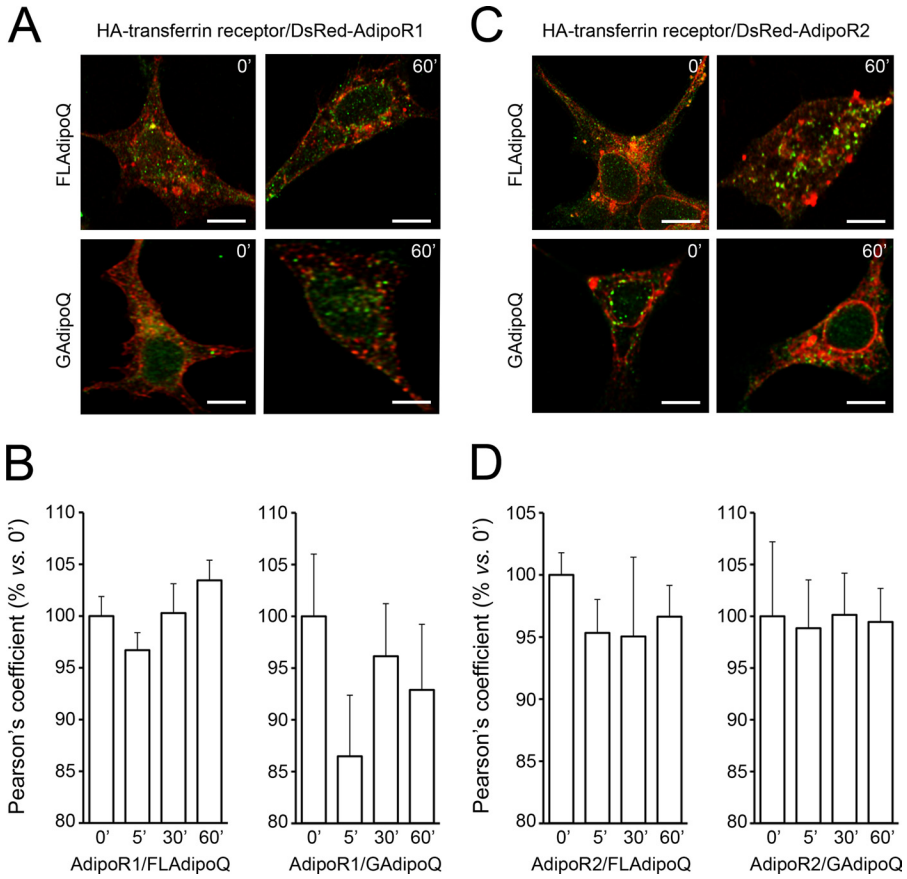

FIGURE 6. **AdipoR1 and AdipoR2 internalization dynamics in response to adiponectin.** *A* and *C*, shown are representative confocal images of DsRed-AdipoR1 (*A*)- or DsRed-AdipoR2-expressing (*C*) HEK293AD cells transfected with the recycling endosome marker transferrin receptor tagged with HA (*green*) and treated with 100 nM FLAdipoQ (*left panels*) or 100 nM GAdipoQ (*right panels*) for 0, 5, 30, and 60 min. *Scale bars*, 5 μm. *B* and *D*, shown is quantification of the colocalization index between DsRed-AdipoR1 or DsRed-AdipoR2 and transferrin receptor immunofluorescent signals in FLAdipoQ (*left graphs*)- or GAdipoQ-treated cells (*right graphs*). Data are presented as the average ± S.E. from at least 12 cells per group collected from 3 independent experiments.

immunoprecipitation assays suggested that they might form high-order complexes (16). This was subsequently confirmed for AdipoR1, which was shown to organize into homomers via a *GXXXG* interaction motif in the fifth transmembrane helix (26). Our FRET measurements have further confirmed the capacity of AdipoR1 to form homomers. Furthermore, analysis of normalized FRET images has allowed us to unveil for the first time that AdipoR1 interaction takes place mainly at the plasma membrane. Nevertheless, receptor interaction was also found to occur at the ER, suggesting that AdipoR1 homomerization is initiated early in the secretory pathway.

The FRET efficiency detected for AdipoR1 homomer formation was similar to the theoretical maximal FRET efficiency, which suggests that most AdipoR1 molecules form self-associated complexes under non-stimulated conditions. This finding implies that AdipoR1 dimer formation does not depend on ligand binding, but it is a constitutive feature of this receptor, as it has been also shown to occur for several tyrosine kinase receptors (24) and GPCRs (38). Furthermore, real-time FRET measurement in living cells revealed that FLAdipoQ or GAdipoQ causes a fast decrease in FRET efficiency that suggests the occurrence of conformational changes in AdipoR1 and/or AdipoR1 homomer dissociation upon adiponectin binding, as has been suggested to occur for GPCRs (33, 34). Previously, it was reported that FLAdipoQ treatment decreased the interaction between AdipoR1 receptors, which led to the proposal that ligand binding could prevent the initial association of monomers into dimers (26). These findings were obtained by combining bimolecular fluorescence complementation with flow cytometry, which represents a valuable method to validate protein interactions but does not offer time-resolved dynamics of such processes. On the other hand, our study is based on live FRET imaging, which provides temporal information about the dynamics of receptor complexes (39). Accordingly, our findings suggest that AdipoR1 forms stable homomers under basal conditions but that these complexes may dissociate in response to adiponectin binding. Remarkably, shortly after adiponectin-induced receptor dissociation, FRET efficiencies tended to recover basal levels, suggesting thereby that AdipoR1 could re-associate rapidly into homomers.

Although to date there has not been direct evidence on the ability of AdipoR2 to form oligomeric complexes, the presence of the *GXXXG* dimerization motif in its fifth transmembrane domain suggested that this receptor could also organize into high-order complexes. In line with this notion, our FRET and

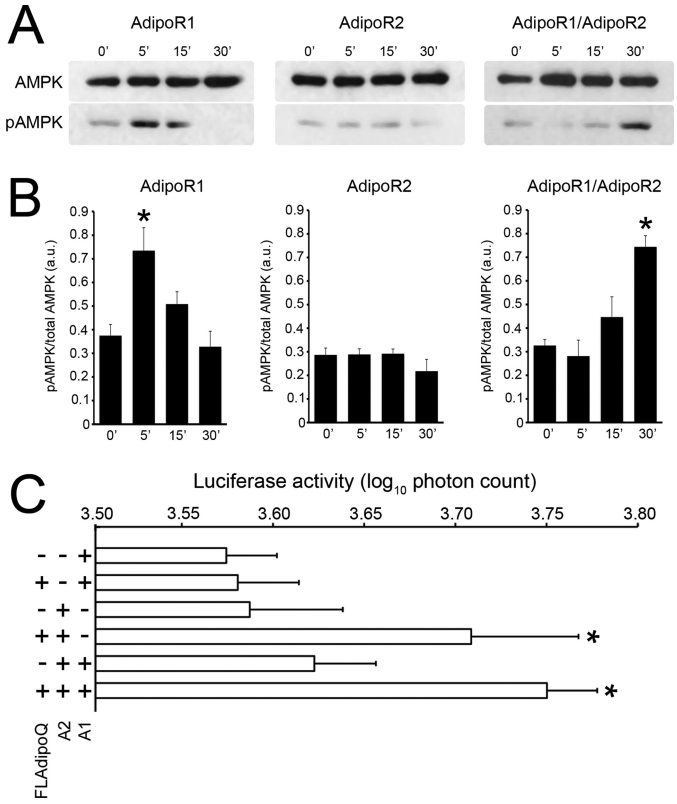

FIGURE 7. **Time-dependent effect of FLAdipoQ treatment on the phosphorylation of AMPK.** *A*, shown are representative blots of HEK293AD cells expressing exogenous AdipoR1 alone (*left panel*), AdipoR2 alone (*middle panel*), or co-expressing AdipoR1 and AdipoR2 (*right panel*). *B*, shown are average band intensities of adiponectin-induced AMPK phosphorylation rates in AdipoR1 (*left graph*)-, AdipoR2 (*middle graph*)-, or AdipoR1/AdipoR2-expressing cells (*right graph*). AMPK phosphorylation was determined as phospho-AMPK normalized by total AMPK and are represented as the average ± S.E. from at least three independent experiments. * $p < 0.001$ *versus* untreated cells. *C*, PPARα activity was measured as the capacity of FLAdipoQ to increase DR1-driven luciferase synthesis. AdipoR1-, AdipoR2-, or AdipoR1/AdipoR2-expressing HepG2 cells were co-transfected with a DR1-luciferase reporter plasmid. Photon emission was assessed in single, living cells under basal conditions and after a 60-min exposure to 100 nM FLAdipoQ. Data are expressed as the $\log_{10}$ of the photon emission integrated in 10-min intervals and are represented as the average ± S.E. from at least 27 cells from 5 independent experiments. *, $p < 0.05$ *versus* untreated cells.

immunoblot experiments demonstrate that AdipoR2 forms homomers under non-stimulated conditions with similar efficiency to that observed for AdipoR1. Likewise, the dissociation and internalization dynamics of AdipoR2 homomers in response to adiponectin are similar to those of AdipoR1. Furthermore, AdipoR2 was also found to self-associate at the plasma membrane and, to a lesser extent, on the ER membranes. Interestingly, the Class C GPCR $GABA_B$ receptor and the Class A GPCRα_{1B}- and β_2-adrenoceptors have been reported to form dimers in the ER (40–42). Furthermore, disruption of the putative dimerization motif of the β_2-adrenergic receptor prevents its normal trafficking to the plasma membrane, indicating that receptor dimerization plays an important role in ER export and cell surface targeting (42). The observation that both AdipoR1 and AdipoR2 homomers localize to the ER strongly suggests that the ER may represent the cellular compartment wherein the organization of AdipoR quaternary structures begins. It is plausible that AdipoR dimerization takes also place in the Golgi apparatus as, at least for class A GPCR, it has been shown that homodimerization/oligomerization of these receptors occurs both in the ER and the Golgi, although not exclusively in the Golgi (43).

Besides forming homomers, AdipoRs undergo efficient heteromeric interactions in non-stimulated cells. Adiponectin binding to AdipoR1/AdipoR2 heteromers may also trigger receptor dissociation, as supported by our live FRET imaging data, although heteromers present a distinct behavior in response to ligand binding as compared with homomers. Specifically, FLAdipoQ would provoke a faster dissociation rate of AdipoR1/AdipoR2 heteromers than of their homomer counterparts. Disruption and disassembly of oligomeric receptors is commonly triggered by ligand-induced changes in receptor conformation. This has been reported for several members of the GPCR superfamily: δ-opioid receptor (44), thyrotropin receptor (45), somatostatin receptor 2 (34, 46), and dopamine receptors (47). Interestingly, dissociation of dopamine receptor heteromers was found to require lower concentrations of dopamine than for the homomeric complexes, which led to the proposal that the interaction between heteromers is weaker than that maintaining the homomeric conformations (47). Similarly, AdipoR heteromers dissociated faster than the homomeric forms in response to equimolar concentrations of FLAdipoQ, suggesting that in this case heteromeric interactions could also be less stable than the homomeric ones.

Oligomerization of membrane receptors has been shown to affect receptor function, including ligand binding, signaling, receptor desensitization, and receptor internalization (34, 38, 44, 48–50). Accordingly, we first explored whether the different AdipoR complexes internalize differently upon FLAdipoQ or GAdipoQ binding. We found that both AdipoR1 and AdipoR2 redistribute to early endosomes in response to either FLAdipoQ or GAdipoQ, which suggests that AdipoR endocytosis is not affected by the composition of the receptor complex. Notably, the amount of internalized receptors relative to those remaining at the cell surface after stimulation was relatively low in response to both ligands. The internalization process was different depending on the adiponectin form administered. Specifically, localization of AdipoRs to early endosomes occurred within the first 5 min after FLAdipoQ administration and disappeared 30 min later. On the other hand, AdipoRs only localized to early endosomes after 30 min of exposure to GAdipoQ. These data indicate that the various forms of adiponectin operate differently on AdipoR complexes, which could in turn affect the endocytic trafficking and signaling of the receptor complex. In this regard it is important to stress that the different forms of adiponectin mediate distinct and often tissue-specific effects (14, 51). Together, these and our findings support the notion that activation of distinct signal transduction pathways by the different adiponectin isoforms is due at least in part to the presence of AdipoR complexes.

After ligand-induced internalization, receptors can be recycled back to the membrane through the early endosome-recycling endosome pathway or directed to lysosomes for degradation. Our co-localization analyses showed that AdipoR1 and AdipoR2 significantly colocalize with the lysosome marker LAMP1 only after a 30–60-min exposure to

FLAdipoQ or GAdipoQ, whereas treatments did not modify the co-localization rate of AdipoRs with transferrin receptor. Altogether, these data indicate that, at least at the conditions tested, most AdipoRs are diverted to the lysosomal-degradation pathway after ligand activation. According to these observations, it is conceivable that the response of cells to adiponectin decreases over time due to AdipoR down-regulation.

Our study also shows that the signaling pathways activated by a given adiponectin isoform may differ depending on the AdipoR repertoire expressed by the cells. To be more specific, given that adiponectin increases phosphorylation and activity of AMPK (52), we investigated the capacity of the different AdipoR complexes to phosphorylate this enzyme. We observed that similarly to that previously reported (52), phosphorylation of AMPK peaked at 5 min in FLAdipoQ-treated, AdipoR1-expressing cells. In fact, our data confirm previous observations indicating that adiponectin-induced activation of AMPK occurs mainly via AdipoR1 (18) inasmuch as FLAdipoQ did not evoke any change in AdipoR2-expressing cells at any of the time points tested. Interestingly, in cells expressing both AdipoR1 and AdipoR2, phosphorylation of AMPK only increased after a 30-min treatment with the adipokine, which indicates that the presence of AdipoR1/AdipoR2 heteromers provokes a delay in the onset of AMPK activation in response to adiponectin. Given that double-transfected cells contain AdipoR1 homomers and AdipoR2 homomers as well as heterodimers, it is plausible that the delayed intracellular response observed in these cells is due to a decrease in the proportion of AdipoR1 homodimers and/or to a lower capacity of the heterodimer to signal through the AMPK pathway as a consequence of the interaction with AdipoR2 and/or the presence of AdipoR2 dimers. Further research is required to ascertain these possibilities.

AdipoR2 is known to initiate an intracellular signal cascade that involves PPARα activation (18), and therefore, we evaluated whether AdipoR heteromer formation affects PPARα signaling. We found that, consistent with previous results (18), FLAdipoQ enhanced PPARα activity in cells expressing AdipoR2 but not AdipoR1. Interestingly, in cells expressing both receptors, FLAdipoQ was able to increase PPARα activity at similar levels than those observed in AdipoR2-expressing cells, suggesting that the presence of heteromers might not alter AdipoR2 intracellular signaling.

It is currently known that both circulating adiponectin and the expression levels of its receptors in target cells are decreased in obesity, which has been suggested to contribute to obesity-associated insulin resistance (53). Three therapeutic strategies targeting adiponectin and its receptors have been currently contemplated to tackle the metabolic and cardiovascular abnormalities commonly linked to obesity: (i) to increase adiponectin expression in white adipose tissue and plasma adiponectin levels using PPARγ agonists (54), (ii) to up-regulate AdipoR expression using PPARα agonists (55), and (iii) to characterize novel AdipoR agonists to counteract obesity-associated reduced adiponectin sensitivity (56). In the present study, we have demonstrated that AdipoR1 and AdipoR2 interact to form homomers and heteromers that exhibit distinct adiponectin binding affinities and intracellular signaling properties. Therefore, the balance of AdipoR homomers and heteromers in target tissues must be taken into account when envisaging adiponectin-based treatments regardless of the therapeutic strategy chosen.

Acknowledgments—We are indebted to Dr. Youssef Anouar from the European Institute for Peptide Research, University of Rouen, France, for the generous gift of the pCMV-cMyc vector and Dr. Jae Bum Kim from the laboratory of Adipocyte and Metabolism Research, Research Center for Functional Cellulomics, Department of Biological Sciences, Seoul National University, Seoul, Korea, for providing the DR1-luciferase vector. We thank Esther Peralbo Santaella (Instituto Maimonides de Investigacion Biomedica de Cordoba) and Laura Molero (CIBER Fisiopatologia de la Obesidad y Nutricion) for technical assistance.

REFERENCES

1. Rajala, M. W., and Scherer, P. E. (2003) Minireview. The adipocyte. At the crossroads of energy homeostasis, inflammation, and atherosclerosis. *Endocrinology* **144,** 3765–3773
2. Scherer, P. E., Williams, S., Fogliano, M., Baldini, G., and Lodish, H. F. (1995) A novel serum protein similar to C1q, produced exclusively in adipocytes. *J. Biol. Chem.* **270,** 26746–26749
3. Hu, E., Liang, P., and Spiegelman, B. M. (1996) AdipoQ is a novel adipose-specific gene dysregulated in obesity. *J. Biol. Chem.* **271,** 10697–10703
4. Maeda, K., Okubo, K., Shimomura, I., Funahashi, T., Matsuzawa, Y., and Matsubara, K. (1996) cDNA cloning and expression of a novel adipose specific collagen-like factor, apM1 (AdiPose most abundant gene transcript 1). *Biochem. Biophys. Res. Commun.* **221,** 286–289
5. Nakano, Y., Tobe, T., Choi-Miura, N. H., Mazda, T., and Tomita, M. (1996) Isolation and characterization of GBP28, a novel gelatin-binding protein purified from human plasma. *J. Biochem.* **120,** 803–812
6. Kadowaki, T., and Yamauchi, T. (2005) Adiponectin and adiponectin receptors. *Endocr. Rev.* **26,** 439–451
7. Hui, X., Lam, K. S., Vanhoutte, P. M., and Xu, A. (2012) Adiponectin and cardiovascular health. An update. *Br. J. Pharmacol.* **165,** 574–590
8. Maenhaut, N., and Van de Voorde, J. (2011) Regulation of vascular tone by adipocytes. *BMC Med.* **9,** 25
9. Ouchi, N., Parker, J. L., Lugus, J. J., and Walsh, K. (2011) Adipokines in inflammation and metabolic disease. *Nat. Rev. Immunol.* **11,** 85–97
10. Xu, A., and Vanhoutte, P. M. (2012) Adiponectin and adipocyte fatty acid binding protein in the pathogenesis of cardiovascular disease. *Am. J. Physiol. Heart Circ. Physiol.* **302,** H1231–H1240
11. Holland, W. L., Miller, R. A., Wang, Z. V., Sun, K., Barth, B. M., Bui, H. H., Davis, K. E., Bikman, B. T., Halberg, N., Rutkowski, J. M., Wade, M. R., Tenorio, V. M., Kuo, M. S., Brozinick, J. T., Zhang, B. B., Birnbaum, M. J., Summers, S. A., and Scherer, P. E. (2011) Receptor-mediated activation of ceramidase activity initiates the pleiotropic actions of adiponectin. *Nat. Med.* **17,** 55–63
12. Chen, X., and Wang, Y. (2011) Adiponectin and breast cancer. *Med. Oncol.* **28,** 1288–1295
13. Dalamaga, M., Diakopoulos, K. N., and Mantzoros, C. S. (2012) The role of adiponectin in cancer. A review of current evidence. *Endocr. Rev.* **33,** 547–594
14. Tsao, T. S., Tomas, E., Murrey, H. E., Hug, C., Lee, D. H., Ruderman, N. B., Heuser, J. E., and Lodish, H. F. (2003) Role of disulfide bonds in Acrp30/adiponectin structure and signaling specificity. Different oligomers activate different signal transduction pathways. *J. Biol. Chem.* **278,** 50810–50817
15. Waki, H., Yamauchi, T., Kamon, J., Kita, S., Ito, Y., Hada, Y., Uchida, S., Tsuchida, A., Takekawa, S., and Kadowaki, T. (2005) Generation of globular fragment of adiponectin by leukocyte elastase secreted by monocytic

cell line THP-1. *Endocrinology* **146,** 790–796
16. Yamauchi, T., Kamon, J., Ito, Y., Tsuchida, A., Yokomizo, T., Kita, S., Sugiyama, T., Miyagishi, M., Hara, K., Tsunoda, M., Murakami, K., Ohteki, T., Uchida, S., Takekawa, S., Waki, H., Tsuno, N. H., Shibata, Y., Terauchi, Y., Froguel, P., Tobe, K., Koyasu, S., Taira, K., Kitamura, T., Shimizu, T., Nagai, R., and Kadowaki, T. (2003) Cloning of adiponectin receptors that mediate antidiabetic metabolic effects. *Nature* **423,** 762–769
17. Buechler, C., Wanninger, J., and Neumeier, M. (2010) Adiponectin receptor binding proteins. Recent advances in elucidating adiponectin signalling pathways. *FEBS Lett.* **584,** 4280–4286
18. Yamauchi, T., Nio, Y., Maki, T., Kobayashi, M., Takazawa, T., Iwabu, M., Okada-Iwabu, M., Kawamoto, S., Kubota, N., Kubota, T., Ito, Y., Kamon, J., Tsuchida, A., Kumagai, K., Kozono, H., Hada, Y., Ogata, H., Tokuyama, K., Tsunoda, M., Ide, T., Murakami, K., Awazawa, M., Takamoto, I., Froguel, P., Hara, K., Tobe, K., Nagai, R., Ueki, K., and Kadowaki, T. (2007) Targeted disruption of AdipoR1 and AdipoR2 causes abrogation of adiponectin binding and metabolic actions. *Nat. Med.* **13,** 332–339
19. Lee, M. H., Klein, R. L., El-Shewy, H. M., Luttrell, D. K., and Luttrell, L. M. (2008) The adiponectin receptors AdipoR1 and AdipoR2 activate ERK1/2 through a Src/Ras-dependent pathway and stimulate cell growth. *Biochemistry* **47,** 11682–11692
20. Iwabu, M., Yamauchi, T., Okada-Iwabu, M., Sato, K., Nakagawa, T., Funata, M., Yamaguchi, M., Namiki, S., Nakayama, R., Tabata, M., Ogata, H., Kubota, N., Takamoto, I., Hayashi, Y. K., Yamauchi, N., Waki, H., Fukayama, M., Nishino, I., Tokuyama, K., Ueki, K., Oike, Y., Ishii, S., Hirose, K., Shimizu, T., Touhara, K., and Kadowaki, T. (2010) Adiponectin and AdipoR1 regulate PGC-1α and mitochondria by Ca^{2+} and AMPK/SIRT1. *Nature* **464,** 1313–1319
21. Zhou, L., Deepa, S. S., Etzler, J. C., Ryu, J., Mao, X., Fang, Q., Liu, D. D., Torres, J. M., Jia, W., Lechleiter, J. D., Liu, F., and Dong, L. Q. (2009) Adiponectin activates AMP-activated protein kinase in muscle cells via APPL1/LKB1-dependent and phospholipase C/Ca^{2+}/Ca^{2+}/calmodulin-dependent protein kinase kinase-dependent pathways. *J. Biol. Chem.* **284,** 22426–22435
22. Heiker, J. T., Wottawah, C. M., Juhl, C., Kosel, D., Mörl, K., and Beck-Sickinger, A. G. (2009) Protein kinase CK2 interacts with adiponectin receptor 1 and participates in adiponectin signaling. *Cell. Signal.* **21,** 936–942
23. Hug, C., Wang, J., Ahmad, N. S., Bogan, J. S., Tsao, T. S., and Lodish, H. F. (2004) T-cadherin is a receptor for hexameric and high molecular weight forms of Acrp30/adiponectin. *Proc. Natl. Acad. Sci. U.S.A.* **101,** 10308–10313
24. De Meyts, P. (2008) The insulin receptor. A prototype for dimeric, allosteric membrane receptors? *Trends Biochem. Sci.* **33,** 376–384
25. Vilardaga, J. P., Agnati, L. F., Fuxe, K., and Ciruela, F. (2010) G-protein-coupled receptor heteromer dynamics. *J. Cell Sci.* **123,** 4215–4220
26. Kosel, D., Heiker, J. T., Juhl, C., Wottawah, C. M., Blüher, M., Mörl, K., and Beck-Sickinger, A. G. (2010) Dimerization of adiponectin receptor 1 is inhibited by adiponectin. *J. Cell Sci.* **123,** 1320–1328
27. Chen, H., Puhl, H. L., 3rd, Koushik, S. V., Vogel, S. S., and Ikeda, S. R. (2006) Measurement of FRET efficiency and ratio of donor to acceptor concentration in living cells. *Biophys. J.* **91,** L39–L41
28. Feige, J. N., Sage, D., Wahli, W., Desvergne, B., and Gelman, L. (2005) PixFRET, an ImageJ plug-in for FRET calculation that can accommodate variations in spectral bleed-throughs. *Microsc. Res. Tech.* **68,** 51–58
29. Gordon, G. W., Berry, G., Liang, X. H., Levine, B., and Herman, B. (1998) Quantitative fluorescence resonance energy transfer measurements using fluorescence microscopy. *Biophys. J.* **74,** 2702–2713
30. Xia, Z., and Liu, Y. (2001) Reliable and global measurement of fluorescence resonance energy transfer using fluorescence microscopes. *Biophys. J.* **81,** 2395–2402
31. Vilardaga, J. P., Bünemann, M., Krasel, C., Castro, M., and Lohse, M. J. (2003) Measurement of the millisecond activation switch of G protein-coupled receptors in living cells. *Nat. Biotechnol.* **21,** 807–812
32. Heyduk, T. (2002) Measuring protein conformational changes by FRET/LRET. *Curr. Opin. Biotechnol.* **13,** 292–296
33. Cheng, Z. J., and Miller, L. J. (2001) Agonist-dependent dissociation of oligomeric complexes of G protein-coupled cholecystokinin receptors demonstrated in living cells using bioluminescence resonance energy transfer. *J. Biol. Chem.* **276,** 48040–48047
34. Grant, M., Collier, B., and Kumar, U. (2004) Agonist-dependent dissociation of human somatostatin receptor 2 dimers. A role in receptor trafficking. *J. Biol. Chem.* **279,** 36179–36183
35. Pin, J. P., Neubig, R., Bouvier, M., Devi, L., Filizola, M., Javitch, J. A., Lohse, M. J., Milligan, G., Palczewski, K., Parmentier, M., and Spedding, M. (2007) International Union of Basic and Clinical Pharmacology. LXVII. Recommendations for the recognition and nomenclature of G protein-coupled receptor heteromultimers. *Pharmacol. Rev.* **59,** 5–13
36. Milligan, G. (2009) G protein-coupled receptor hetero-dimerization. Contribution to pharmacology and function. *Br J. Pharmacol.* **158,** 5–14
37. Rovira, X., Pin, J. P., and Giraldo, J. (2010) The asymmetric/symmetric activation of GPCR dimers as a possible mechanistic rationale for multiple signalling pathways. *Trends Pharmacol. Sci.* **31,** 15–21
38. Bai, M. (2004) Dimerization of G-protein-coupled receptors: roles in signal transduction. *Cell. Signal.* **16,** 175–186
39. Zeug, A., Woehler, A., Neher, E., and Ponimaskin, E. G. (2012) Quantitative intensity-based FRET approaches. A comparative snapshot. *Biophys. J.* **103,** 1821–1827
40. White, J. H., Wise, A., Main, M. J., Green, A., Fraser, N. J., Disney, G. H., Barnes, A. A., Emson, P., Foord, S. M., and Marshall, F. H. (1998) Heterodimerization is required for the formation of a functional GABA(B) receptor. *Nature* **396,** 679–682
41. Margeta-Mitrovic, M., Jan, Y. N., and Jan, L. Y. (2000) A trafficking checkpoint controls GABA(B) receptor heterodimerization. *Neuron* **27,** 97–106
42. Salahpour, A., Angers, S., Mercier, J. F., Lagacé, M., Marullo, S., and Bouvier, M. (2004) Homodimerization of the β2-adrenergic receptor as a prerequisite for cell surface targeting. *J. Biol. Chem.* **279,** 33390–33397
43. Herrick-Davis, K., Weaver, B. A., Grinde, E., and Mazurkiewicz, J. E. (2006) Serotonin 5-HT2C receptor homodimer biogenesis in the endoplasmic reticulum. Real-time visualization with confocal fluorescence resonance energy transfer. *J. Biol. Chem.* **281,** 27109–27116
44. Cvejic, S., and Devi, L. A. (1997) Dimerization of the delta opioid receptor. Implication for a role in receptor internalization. *J. Biol. Chem.* **272,** 26959–26964
45. Latif, R., Graves, P., and Davies, T. F. (2002) Ligand-dependent inhibition of oligomerization at the human thyrotropin receptor. *J. Biol. Chem.* **277,** 45059–45067
46. Durán-Prado, M., Malagón, M. M., Gracia-Navarro, F., and Castaño, J. P. (2008) Dimerization of G protein-coupled receptors: new avenues for somatostatin receptor signalling, control, and functioning. *Mol. Cell. Endocrinol.* **286,** 63–68
47. O'Dowd, B. F., Ji, X., Alijaniaram, M., Nguyen, T., and George, S. R. (2011) Separation and reformation of cell surface dopamine receptor oligomers visualized in cells. *Eur. J. Pharmacol.* **658,** 74–83
48. Carman, C. V., and Benovic, J. L. (1998) G-protein-coupled receptors. Turn-ons and turn-offs. *Curr. Opin. Neurobiol.* **8,** 335–344
49. Tsao, P., Cao, T., and von Zastrow, M. (2001) Role of endocytosis in mediating down-regulation of G-protein-coupled receptors. *Trends Pharmacol. Sci.* **22,** 91–96
50. Tsao, P. I., and von Zastrow, M. (2000) Type-specific sorting of G protein-coupled receptors after endocytosis. *J. Biol. Chem.* **275,** 11130–11140
51. Vu, V., Riddell, M. C., and Sweeney, G. (2007) Circulating adiponectin and adiponectin receptor expression in skeletal muscle. effects of exercise. *Diabetes Metab. Res. Rev.* **23,** 600–611
52. Yamauchi, T., Kamon, J., Minokoshi, Y., Ito, Y., Waki, H., Uchida, S., Yamashita, S., Noda, M., Kita, S., Ueki, K., Eto, K., Akanuma, Y., Froguel, P., Foufelle, F., Ferre, P., Carling, D., Kimura, S., Nagai, R., Kahn, B. B., and Kadowaki, T. (2002) Adiponectin stimulates glucose utilization and fatty acid oxidation by activating AMP-activated protein kinase. *Nat. Med.* **8,** 1288–1295
53. Yamauchi, T., and Kadowaki, T. (2008) Physiological and pathophysiological roles of adiponectin and adiponectin receptors in the integrated regulation of metabolic and cardiovascular diseases. *Int. J. Obes.* **32,** S13–S18
54. Kubota, N., Terauchi, Y., Kubota, T., Kumagai, H., Itoh, S., Satoh, H., Yano, W., Ogata, H., Tokuyama, K., Takamoto, I., Mineyama, T., Ishikawa,

M., Moroi, M., Sugi, K., Yamauchi, T., Ueki, K., Tobe, K., Noda, T., Nagai, R., and Kadowaki, T. (2006) Pioglitazone ameliorates insulin resistance and diabetes by both adiponectin-dependent and -independent pathways. *J. Biol. Chem.* **281,** 8748–8755

55. Tsuchida, A., Yamauchi, T., Takekawa, S., Hada, Y., Ito, Y., Maki, T., and Kadowaki, T. (2005) Peroxisome proliferator-activated receptor PPARα activation increases adiponectin receptors and reduces obesity-related inflammation in adipose tissue. Comparison of activation of PPARα, PPARγ, and their combination. *Diabetes* **54,** 3358–3370
56. Narasimhan, M. L., Coca, M. A., Jin, J., Yamauchi, T., Ito, Y., Kadowaki, T., Kim, K. K., Pardo, J. M., Damsz, B., Hasegawa, P. M., Yun, D. J., and Bressan, R. A. (2005) Osmotin is a homolog of mammalian adiponectin and controls apoptosis in yeast through a homolog of mammalian adiponectin receptor. *Mol. Cell* **17,** 171–180